

Split-sideband spectroscopy in slowly modulated optomechanics

E. B. Aranas, P. G. Z. Fonseca, P. F. Barker and T. S. Monteiro*
*Department of Physics and Astronomy, University College London,
 Gower Street, London WC1E 6BT, United Kingdom*

Optomechanical coupling between the motion of a mechanical oscillator and a cavity represents a new arena for experimental investigation of quantum effects on the mesoscopic and macroscopic scale. The motional sidebands of the output of a cavity offer ultra-sensitive probes of the dynamics. We introduce a scheme whereby these sidebands split asymmetrically and show how they may be used as experimental diagnostics and signatures of quantum noise limited dynamics. We show split-sidebands with controllable asymmetry occur by simultaneously modulating the light-mechanical coupling g and ω_M - slowly and out-of-phase. Such modulations are generic but already occur in optically trapped set-ups where the equilibrium point of the oscillator is varied cyclically. We analyse recently observed, but overlooked, experimental split-sideband asymmetries; although not yet in the quantum regime, the data suggests that split sideband structures are easily accessible to future experiments.

Cavity optomechanics offers rich possibilities for experimental investigation of the theory of quantum measurement and the role of quantum noise [1, 2]. Several groups have successfully cooled a mechanical oscillator via its coupling to a mode of an electromagnetic cavity [3–5] down to its quantum ground state (or very close to it) i.e. mean phonon occupancy $n_{ph} \lesssim 1$. Read-out of the temperature was achieved by detection of motional sidebands in the cavity output; the theory for quantum sidebands was elucidated in [6, 7]. The cavity fields serve a dual purpose: they provide not only the laser cooling but also an ultrasensitive means for detection of displacements on the scale of quantum zero-point fluctuations; this has motivated considerable interest in quantum-limited measurements in this context, following the early pioneering work by Braginsky and Khalili [8].

An important development was the detection of an asymmetry [9–11] in the two frequency peaks (sidebands) of the output power of a probe beam detuned to the positive and negative side of the cavity resonance. Albeit indirectly [10, 11], the observations mirror an underlying asymmetry in the motional spectrum: an oscillator in its ground state $n_{ph} = 0$, can absorb a phonon and down-convert the photon frequency (Stokes process); but it can no longer emit any energy and up-convert a photon (anti-Stokes process).

Sideband asymmetry has become an important tool in optomechanics and has now been used to establish cooling limited by only quantum backaction [12]. Ponderomotive squeezing, whereby narrowband cavity output falls below the technical imprecision noise floor is also of much current interest [13–15] though is also observed in oscillators in a high thermal state.

Recent rapid progress on cooling optically levitated systems suggests ground state cooling may be in sight [16–18]. This strongly motivates development of robust probes of the quantum dynamics. Such systems offer unique potential to sensitively probe quantum noises due to their near complete decoupling from environmen-

tal heating and decoherence. They also readily access the quantum shot-noise limit [17], since in a vacuum, the mechanical damping $\Gamma_M \rightarrow 0$.

A standard optomechanical system comprises a mechanical oscillator interacting with a laser-driven cavity. In the frame rotating with the driving laser, typical experimental regimes using an extraordinarily broad range of physical platforms (cantilevers, microtoroids, membranes, photonic crystals) are well described by the two-coupled oscillator Hamiltonian:

$$\hat{H}/\hbar = \Delta \hat{a}^\dagger \hat{a} + \omega_M (\hat{p}^2 + \hat{x}^2) + g(\hat{a}^\dagger + \hat{a})\hat{x}. \quad (1)$$

\hat{a}^\dagger, \hat{a} are creation and annihilation operators for small fluctuations cavity mode about its equilibrium value α while $\hat{x} \equiv \hat{b} + \hat{b}^\dagger$ (in appropriately scaled units) represents a small displacement of the mechanical oscillator about its equilibrium position x_0 . Dissipative processes are treated by standard input-output theory, including input noises incident in the optical cavity $\sqrt{\kappa}\hat{a}_{in}, \sqrt{\kappa}\hat{a}_{in}^\dagger$ and mechanical oscillator $\sqrt{\Gamma_M}\hat{b}_{in}, \sqrt{\Gamma_M}\hat{b}_{in}^\dagger$ where κ, Γ_M are the cavity and mechanical damping rates while g is the strength of the optomechanical coupling.

However, here we consider instead a harmonically modulated optomechanical coupling $g(t) = 2\bar{g}\sin\omega_d t$ and mechanical frequency $\omega_M(t) = \bar{\omega}_M + 2\omega_2 \cos 2\omega_d t$. Other studies have investigated periodically modulated optomechanics, but interest has been focused on *resonant* driving $\omega_d \sim \omega_M, |\Delta|$ [19, 20] leading to interesting effects like squeezing or OMIT [21]. In contrast, here we investigate systems which are modulated slowly $\bar{\omega}_M \gg \omega_d$ (so as to preserve linearisation about $x_0(t)$ and α) and hence are far off-resonant. In addition, the g, ω_M modulations are out of phase, in the sense that when the mechanical frequency is a maximum, the magnitude of coupling strength between motion and cavity field is a minimum; and vice-versa.

Added impetus to our study is provided by its relevance to optically trapped systems including levitated

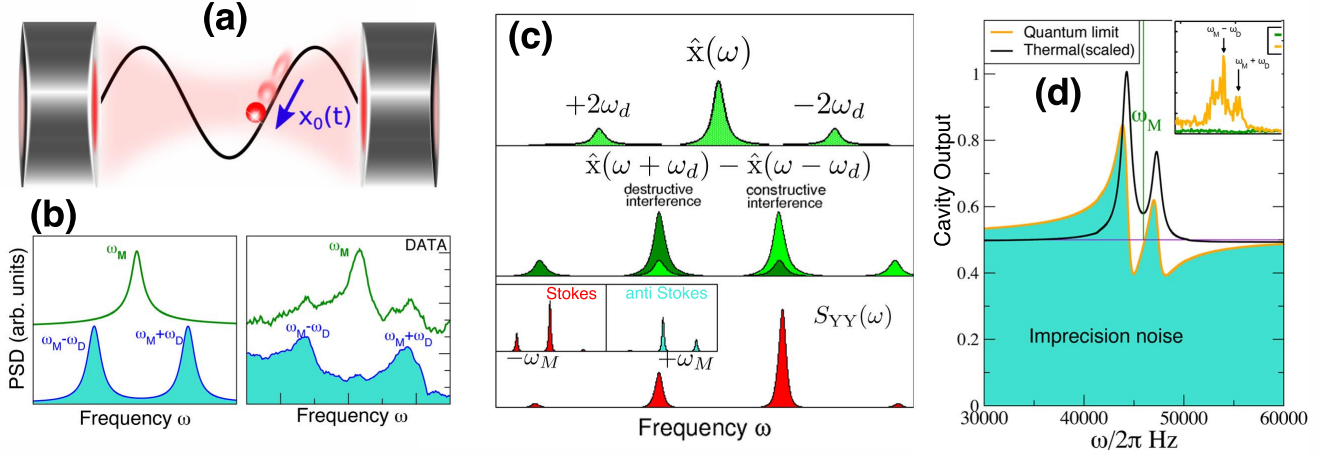


FIG. 1: **(a)** For set-ups where an oscillator is dipole-force trapped by the standing wave of a cavity mode there is no optomechanical cooling at the antinode $x_0 = 0$ (the potential minimum of an optical well of width $\lambda/2$), since there is no light-matter coupling. Hence, such set-ups [26, 29] require an auxiliary field to pull the centre of the mechanical oscillation away from $x_0 = 0$. In electro-optical traps [29], a slow oscillation is induced such that $x_0(t) = X_d \sin \omega_d t$. For small oscillations, we show this corresponds to an effective modulation of the coupling $g(t) = 2\bar{g} \sin \omega_d t$ and a simultaneous, out-of-phase, modulation of the mechanical frequency $\omega_M(t) = \bar{\omega}_M + 2\omega_2 \cos(2\omega_d t)$. **(b)** For a small ($X_d \ll \lambda$) modulation, $\omega_2 \approx 0$ and only g is appreciably modulated. In that case, while the displacement spectrum, $S_{xx}(\omega) \equiv \langle |\hat{x}(\omega)|^2 \rangle$, is still peaked at $\pm \omega \simeq \omega_M$, the experimental cavity spectrum, ($S_{yy}(\omega)$) exhibits a characteristic structure of “twin peaks” at $\pm \omega = \omega_M \pm \omega_d$ [16]. **(c)** For larger modulations, the effect of $\omega_2 > 0$ is to produce additional $\pm 2\omega_d$ side-peaks in the $\hat{x}(\omega)$ spectrum. There is constructive enhancement of the $\omega_M - \omega_d$ peak, and destructive cancellation of the $\omega_M + \omega_d$ peak, so the “twin peak” structure is replaced by a pair of peaks of asymmetric heights. For small \bar{g} , the ratio between peaks $r \simeq (\omega_2 - 2\omega_d)^2 / (\omega_2 + 2\omega_d)^2$ so the $\omega_M + \omega_d$ peak is strongly suppressed for $\omega_2 \sim 2\omega_d$ ($r \approx 0$). This asymmetry is distinct from the usual Stokes/antiStokes sideband asymmetry at $\pm \omega \simeq \omega_M$, which is still present. **(d)** In thermal regimes, the ratio r is insensitive to Γ_M ; however, as $\Gamma_M \rightarrow 0$ and the backaction limit is attained, correlations between back-action and incoming noise alters the relative heights of the peaks, mainly since ponderomotive squeezing lowers the height of the $\omega_M + \omega_d$ peak relative to the imprecision floor. For incoming quantum shot noise, significant changes in r arise only if the oscillator is near the ground state. Inset reproduces (classical) data from Fig.5 of [29] which supports our model of the split-sidebands.

nanoparticles [22–28]. We show here that the anti-phase g, ω_M modulation arises automatically if the mean position of the oscillator varies harmonically $x_0(t) = X_D \sin \omega_d t$. We find it accounts for previously unexplained asymmetries in the sidebands of levitated oscillators, nanoparticles in hybrid electrical-optical traps [16, 29]. Such traps to date provide the only experimental realisation of stable trapping and cooling of a nanoparticle at high vacuum, in a cavity. When strongly cooled, the linearised dynamics of Eq.1 dominate the dynamics [16]. We emphasize the results of the study are generic to any set-up that can achieve these anti-phase g, ω_M modulations; but we illustrate and test the model against numerics used to simulate hybrid trap dynamics [16] and optically trapped particles, as illustrated in Fig.1(a).

The equations of motion for the standard set-up Eq.1 are solved [1] in frequency space. In terms of quadrature operators $\hat{y}(\omega) = \frac{1}{\sqrt{2}} (\hat{a}^\dagger(\omega) + \hat{a}(\omega))$ one may write:

$$\hat{y}(\omega) = ig\eta(\omega) \cdot \hat{x}(\omega) + \sqrt{\kappa} \hat{Y}_{th}(\omega) \quad (2)$$

where $\eta(\omega) = \chi_o(\omega) - \chi_o^*(-\omega)$ and $\hat{Y}_{th}(\omega) = \chi_o(\omega) \hat{a}_{in} + \chi_o^*(-\omega) \hat{a}_{in}^\dagger$, while $\chi_o(\omega) = [-i(\omega + \Delta) + \frac{\kappa}{2}]^{-1}$ represents the optical susceptibility. In this well-known form,

the first term represents the back-action of the mechanical motion on the cavity field, the second the cavity-filtered incoming quantum noise. The measurable, cavity output spectrum is then obtained from input-output theory [1] $\hat{a}_{out}(\omega) = \hat{a}_{in} - \sqrt{\kappa} \hat{a}(\omega)$ by considering the interference with the incoming (imprecision noise, typically shot noise from the laser), so $\hat{y}_{out}(\omega) = \frac{1}{\sqrt{2}} [\hat{a}_{out}(\omega) + \hat{a}_{out}^\dagger(\omega)]$.

If we include the modulation of $g(t)$ we obtain instead:

$$\hat{y}(\omega) = \bar{g}\eta(\omega) \cdot [\hat{x}(\omega + \omega_d) - \hat{x}(\omega - \omega_d)] + \sqrt{\kappa} \hat{Y}_{th}(\omega) \quad (3)$$

We elucidate details in [30], but the notable difference between the standard case and the modulated optomechanics is that in Eq.3 the optical field does not probe the displacement spectrum $\hat{x}(\omega)$ but rather is sensitive to the interference between shifted spectra at $\omega_M \pm \omega_d$.

For $\omega_2 \simeq 0$, the minus sign in Eq.3 is not significant: the shifted spectra do not interfere appreciably. The result is a cavity field fluctuation spectrum characterised by a “twin peaks” structure as illustrated in Fig.1(b) and also in [16]. The green trace shows the phase of the Pound-Drever-Hall signal used to lock the cavity: while not a sensitive detection method, it follows the phase of

the field so more directly represents $\hat{x}(\omega)$: the latter is peaked at $\omega = \omega_M$, in contrast with the cavity intensity modulations which are peaked at $\omega_M \pm \omega_d$.

The effect of the frequency modulation, $\omega_M(t) = \bar{\omega}_M + 2\omega_2 \cos 2\omega_d t$ however, is to couple $\hat{x}(\omega)$ directly to $\hat{x}(\omega \pm 2\omega_d)$; in that case, $\hat{x}(\omega)$ acquires corresponding sidebands which, as illustrated in Fig.1(c), cause the two main peaks of the shifted spectra $\hat{X}^\pm(\omega) = \hat{x}(\omega + \omega_d) - \hat{x}(\omega - \omega_d)$ to interfere with each other's sidebands. In this case, the minus sign in Eq.3 (and the out-of-phase nature of the modulations) implies that one peak grows by constructive interference, while the other one diminishes.

Full details are in [30], but this can be understood from a simple argument. For modest backaction (\bar{g} small), we can write $\hat{X}^\pm(\omega)$ in the form:

$$\hat{X}^\pm(\omega) \approx \sqrt{\Gamma_M}[\hat{X}_{th}(\omega + \omega_d) - \hat{X}_{th}(\omega - \omega_d)] + \bar{g}\hat{Y}_{BA}(\omega) - i\omega_2\sqrt{\Gamma_M}\hat{X}_{\omega_2}(\omega) - i\omega_2\bar{g}\hat{Y}_{BA}^{(\omega_2)}(\omega) \quad (4)$$

where the \hat{X}_{th} terms represent incoming thermal noises, \hat{Y}_{BA} represents the back-action terms driven by imprecision noise. The last two terms are corrections to account for the modulation of ω_M ; the first comprises thermal effects, the second the corresponding back-action effects.

For $\omega_2 = 0$ and neglecting backaction, the shifted spectra arise mainly from incoming thermal noises $\hat{X}_{th}(\omega) = \chi_M(\omega)\hat{b}_{in} + \chi_M^*(-\omega)\hat{b}_{in}^\dagger$ weighted by the mechanical susceptibility $\chi_M(\omega) = [-i(\omega - \omega_M) + \frac{\Gamma_M}{2}]^{-1}$. The anti-Stokes sideband for example, is primarily due to the weighted thermal noise operators $\chi_M(\omega \pm \omega_d)\hat{b}_{in}(\omega \pm \omega_d)$. The susceptibilities $|\chi_M(\omega \pm \omega_d)|$ are sharply peaked at frequencies $\omega = \omega_M \mp \omega_d$ (since Γ_M is small), yielding the “twin peaks” structure since the ratio of the twin peak weights $r = |\chi_M(\omega - \omega_d)|^2/|\chi_M(\omega + \omega_d)|^2 = 1$.

The main effect of ω_2 is to introduce the extra correction from the \hat{X}_{ω_2} term which means replacing the thermal weights:

$$\chi_M(\omega \pm \omega_d) \rightarrow \chi_M(\omega \pm \omega_d)[1 - i\omega_2\chi_M(\omega \mp \omega_d)] \quad (5)$$

Evaluating the corrections (the terms in square brackets) near the frequency peaks of the noise, we find they are $\approx (2\omega_d \pm \omega_2)/2\omega_d$ so the ratio of peaks in the PSD would be:

$$r \approx (2\omega_d - \omega_2)^2/(2\omega_d + \omega_2)^2, \quad (6)$$

predicting a full cancellation for $2\omega_d \sim \omega_2$.

For the standard optomechanical equations, Eq.2 and its $\hat{x}(\omega)$ equivalent are solved to obtain $S_{XX}(\omega)$ and $S_{yy}(\omega)$ or $S_{y_{out}y_{out}}(\omega)$ in closed form.

However, for the modulated spectra this is not possible: $\hat{y}(\omega)$ depends on shifted $\hat{x}(\omega)$ spectra; and the ω_2

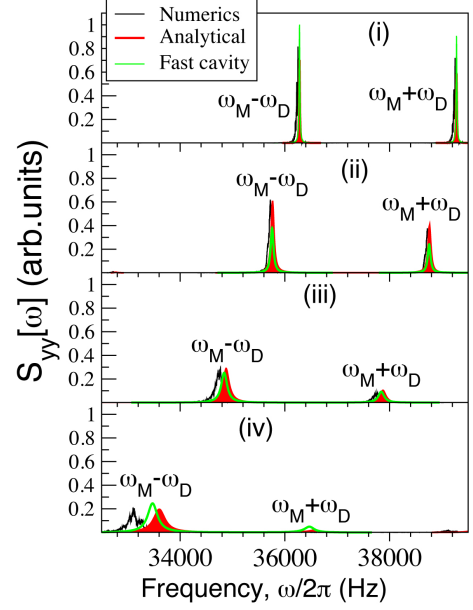


FIG. 2: Comparison of the analytical split-sideband calculations with stochastic numerics and fast cavity model, with increasing \bar{g}, ω_2 for an optically trapped particle for thermal spectra, far from the quantum limit. Here, peak heights scale with Γ_M and r is independent of Γ_M . In this regime, to obtain $S_{yy}(\omega)$ in units of Hz^{-1} , for arbitrary Γ_M , graphs should be scaled as $S_{yy}(\omega) \times \Gamma_M/0.8$; in turn, for the optically trapped nanoparticles in [16], $\Gamma_M \simeq 0.2 \times 10^4 P$, where the gas pressure ranges from $P = 1 - 10^{-8}$ mbar. $\kappa/2 = 130 \times 2\pi$ kHz, $\Delta \simeq -75 \times 2\pi$ kHz. Parameters are far from the sideband-resolved limit, so the fast-cavity model also gives reasonable results. $N = 100, 200, 300, 400$ in Eq.8 hence (i) $\omega_2/2\omega_d = 0.05$, $\bar{g} = 8500\text{s}^{-1}$ (ii) $\omega_2/2\omega_d = 0.2$, $\bar{g} = 17000\text{s}^{-1}$ (iii) $\omega_2/2\omega_d = 0.5$, $\bar{g} = 25000\text{s}^{-1}$, (iv) $\omega_2/2\omega_d = 0.9$, $\bar{g} = 33000\text{s}^{-1}$.

modulation couples $\hat{x}(\omega)$ spectra to the displacement spectra $\hat{x}(\omega \pm 2\omega_d)$. Eqs.3 and 4 are instead solved iteratively, assuming $\bar{g}, \omega_2 \ll \kappa, \omega_M$ and retaining terms up to cubic order in \bar{g}, ω_2 (see [30]). In the thermal regime, the resulting equations are tested against a set of numerical stochastic equations and another model, used to simulate optically trapped particles [16, 29], as seen in Fig.2.

We then take $\Gamma_M \rightarrow 0$ which for cooling parameters (red-detuned light) takes the system down to the quantum backaction limit, where the heating is limited by quantum shot noise, $n_{ph} \equiv n_{BA} \approx (\frac{\kappa}{4\omega_M})^2$ [12]. When we calculate $S_{X^\pm X^\pm}$ (the PSD for $\hat{X}^\pm(\omega)$), we find that it differs very little from the thermal spectrum. This indicates that even for $\Gamma_M = 0$, a regime where the oscillator motion is completely driven by the incoming optical imprecision noise (quantum or classical in fact: this is true for a finite photon temperature), the shape, and r for $S_{X^\pm X^\pm}$ unchanged as shown in Fig.3(a).

However, for $S_{y_{out}y_{out}}(\omega)$, this is not the case: when the same solution used for Fig.3(a) is added and interfered with the incoming (imprecision) optical shot

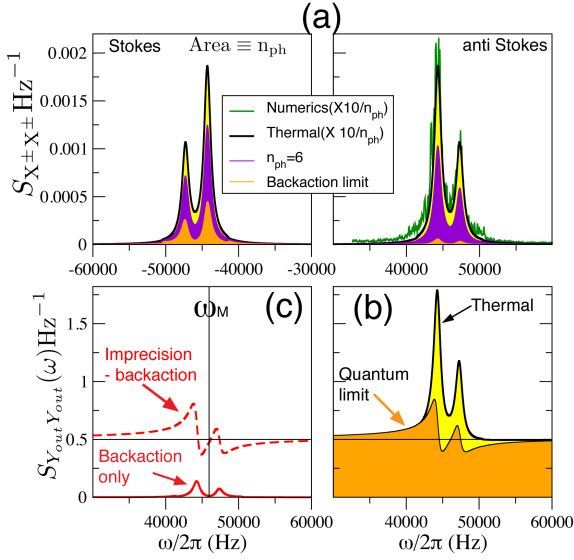


FIG. 3: Comparison between the thermal spectrum and the quantum limit, using the analytical solutions with increasing g, ω_2 in the sideband-resolved limit, which can yield ground state cooling at sufficiently low pressures. (a) Shows $S_{X \pm X \pm}(\omega)$ for Stokes and anti-Stokes sidebands, as $\Gamma_M \rightarrow 0$ while the optomechanical cooling rate Γ_{opt} in each graph remains fixed. The individual sideband shapes are unchanged, but Stokes/anti-Stokes asymmetry develops. The symmetric classical spectra are scaled to a height of 1 corresponding to $\Gamma_M = 10^{-4} \text{ s}^{-1}$. $\omega_2/2\omega_d = 0.24$, for $2\omega_d = 3 \times 2\pi \text{ KHz}$; $g = 18, 500 \text{ s}^{-1}$, $\bar{\omega}_M = 46 \times 2\pi \text{ KHz}$, $\kappa/2 = 26 \times 2\pi \text{ KHz}$, $\Delta \simeq -\omega_M$. (b) The same solutions in (b) are now added to incoming imprecision noise to obtain output spectra $S_{Y_{out} Y_{out}}(\omega)$. At high phonon occupancies, the shape is unchanged. As $n_{ph} \rightarrow n_{BA}$, the ratio above the quantum imprecision floor alters significantly. (c) Shows individual contributions to the PSD; the pure backaction term has the same shape as the thermal split sidebands; its interference with incoming imprecision noise lowers the height of the $\omega_M + \omega_d$ sideband.

noise, the sideband shape is unchanged for the thermal regime but changes significantly in the quantum back-action limit.

The underlying reason for this change can be understood as follows: the total back-action in Eq.4, $\bar{g}\hat{Y}_T(\omega) = \bar{g}[\hat{Y}_{BA}(\omega) - i\omega_2\hat{Y}_{BA}^{(\omega_2)}(\omega)]$, which by itself still yields a ratio of r , develops correlations with the incoming imprecision terms $\hat{Y}_{imp}(\omega) = \hat{a}_{in} + \hat{a}_{in}^\dagger - \sqrt{\kappa}\hat{Y}_{th}$. The key difference seen between $S_{X \pm X \pm}$ and $S_{y_{out} y_{out}}(\omega)$ in the quantum limit, arise because:

$$\langle |\bar{g}\hat{Y}_T(\omega)|^2 \rangle \neq \langle |\frac{\hat{Y}_{imp}(\omega)}{\sqrt{\kappa}} - \bar{g}\hat{Y}_T(\omega)|^2 \rangle \quad (7)$$

The above two terms are contrasted in Fig.3(c). Ponderomotive squeezing originates from such correlations [13–15] between backaction and incoming noise and, in the standard optomechanical case, it leads to a Fano-like line experimental profile [13–15] and (an often small) dip where the output light spectrum lies below the imprecision floor.

However, in the present case, the height of the $\omega_M + \omega_d$ peak is lowered as it overlaps with a ponderomotive squeezing “dip” of the stronger peak as seen in Fig.3(b), leading to a change in r : the sideband structure is more strikingly reshaped and the Γ_M invariance of r is lost. Although ponderomotive squeezing does not require a ground state oscillator, for quantum shot-noise limited spectra, a change in r only becomes appreciable if $n_{ph} \rightarrow n_{BA}$, leading to a noticeable decrease in height of the $\omega_M + \omega_d$ peak above the imprecision noise level. *Stochastic numerical model* As outlined in [16, 29], a nanoparticle in a hybrid electrical-optical trap experiences a dipole force potential $V(x) = -\hbar A|a(t)|^2 \cos^2(kx)$ from the optical standing wave of a cavity (with axis along x). In [16], the depth of the potential $A = 26 \times 2\pi \text{ KHz}$, while the cavity photon number $|a(t)|^2$ fluctuates about mean value of $\approx 10^9 - 10^{10}$ photons; $k = 2\pi/\lambda$ with $\lambda = 1064 \text{ nm}$. The particle becomes trapped in a given optical well N , with anti-node (potential minimum) at $x = X_N$ where $kX_N = 2\pi N$. It experiences also an additional oscillating harmonic potential $V^{AC}(x, t) = \frac{1}{2}m\omega_T^2(x + x_N)^2 \cos(\omega_d t)$ from an ion trap. We test our model by comparing with solutions of the equations of motion in these combined potentials, including also damping for the cavity (κ) and for mechanical degrees of freedom Γ_M) as well as stochastic Gaussian noise to allow for gas collisions and shot noise. This represents a stringent test of our analytical noise model since, in the numerics, \bar{g}, ω_M and ω_2 are not even input parameters: they are themselves emergent properties of the numerical simulations. For $\langle |a(t)|^2 \rangle \equiv \alpha$, we find:

$$\begin{aligned} 2kx_0(t) &\approx -\frac{\omega_T^2}{\omega_M^2}(2kx_N)\sin(\omega_d t) \equiv X_d \sin(\omega_d t) \\ m\omega_M^2 &= 2\hbar k^2 A |\bar{\alpha}|^2 \cos(2kx_0) \\ 2\bar{g} &= kA\bar{\alpha} \sin(2kx_0). \end{aligned} \quad (8)$$

hence the equilibrium point of the oscillations $x_0(t)$ oscillates as $\sin(\omega_d t)$, leading to modulated ω_M, \bar{g} .

The fast mechanical motion $x_M(t) \simeq X_M \cos \Phi_M(t)$ where X_M is the variance of the thermal motion, the phase being $\Phi_M(t) = \int \omega_M(t) dt$.

For a fast cavity, we can assume the cavity field follows $x(t)$ with no delay; to simulate this we combine the slow $x_0(t)$ motion with the fast mechanical motion into the ansatz $x(t) = X_d \sin(\omega_d t) + X_M \cos(\bar{\omega}_M + \frac{\omega_2}{2\omega_d} \sin 2\omega_d t)$. The Fourier transform of $\cos 2kx(t)$ using this ansatz, gives a reasonable approximation of the split-sideband spectrum, for a fast cavity. Fig.2 shows that it yields reasonable agreement with numerics and analysis. More importantly, it describes also scattering of light out of the cavity (illustrated in inset of Fig1(d)) which illustrated suppression of the $\omega_M + \omega_d$ sideband. While not a full demonstration, this classical-regime data does demonstrate the coherent relative phase accumulation and interplay between the slow and fast

motions; it indicates that in combination with homodyne or heterodyne detection, split sideband asymmetries may be investigated experimentally once quantum-limited regimes are attained.

Conclusions Split sideband spectroscopy offers a promising new experimental signature; measurement of the ratio r complements Stokes/antiStokes asymmetry and offers an alternative probe of ponderomotive squeezing. For a system where the back-action spectra is noticeably reshaped by interference with incoming noise, a striking signature of the quantum limit potentially exists in a single sideband, since r is well defined and controllable. Conversely, the double-sidebands may offer an additional diagnostic of Stokes/antiStokes asymmetry as there are two pairs of peaks to compare.

* Electronic address: t.monteiro@ucl.ac.uk

- [1] M. Aspelmeyer, T.J. Kippenberg, F. Marquardt, *Rev. Mod. Phys.* **86**, 1391 (2014).
- [2] A. A. Clerk, M. H. Devoret, S. M. Girvin, Florian Marquardt, and R. J. Schoelkopf *Rev. Mod. Phys.* **82**, 1155 (2010).
- [3] Teufel, J. D., Donner, T., Li, D., Harlow, J. H., Allman, M. S., Cicak, K., Sirois, A. J., Whittaker, J. D., Lehnert, K. W. and Simmonds R. W., *Nature* **475**, 359 (2011).
- [4] Chan, J., Mayer Alegre, T. P., Safavi-Naeini, A. H., Hill, J. T., Krause, A., Groeblacher, S., Aspelmeyer, M. and Painter, O., *Nature* **478**, 89 (2011).
- [5] E. Verhagen, S. Deleglise, S. Weis, A. Schliesser, and T. J. Kippenberg, *Nature* **482**, 63 (2012).
- [6] F. Marquardt, J.P. Chen, A.A. Clerk, S.M. Girvin, *Phys. Rev. Lett.* **99**, 093902 (2007).
- [7] I. Wilson-Rae, N. Nooshi, W. Zwerger, T.J. Kippenberg, *Phys. Rev. Lett.* **99**, 093901 (2007).
- [8] V. Braginsky, F.Y. Khalili, *Quantum Measurement*, Cambridge University Press (1992).
- [9] Amir H. Safavi-Naeini, Jasper Chan, Jeff T. Hill, Thiago P. Mayer Alegre, Alex Krause, and Oskar Painter, *Phys. Rev. Lett.* **108**, 033602 (2012).
- [10] Farid Ya. Khalili, Haixing Miao, Huan Yang, Amir H. Safavi-Naeini, Oskar Painter, Yanbei Chen, *Phys. Rev. A* **86**, 033840 (2012).
- [11] A. J. Weinstein, C. U. Lei, E. E. Wollman, J. Suh, A. Metelmann, A. A. Clerk, and K. C. Schwab, *Phys. Rev. X* **4**, 041003.
- [12] R.W. Peterson, T.P. Purdy, N.S. Kampel, R.W. Andrews, P.-L. Yu, K.W. Lehnert, and C.A. Regal *Phys. Rev. Lett.* **116**, 063601 (2016).
- [13] Safavi-Naeini, A. H., Groblacher, S., Hill, J. T., Chan, J., Aspelmeyer, M. and Painter, O., *Nature* **500**, 185 (2013).
- [14] T.P. Purdy, P.L. Yu, R.W. Peterson, N.S. Kampel, C.A. Regal, *Phys. Rev. X* **3**, 031012 (2013).
- [15] A. Pontin, C. Biancofiore, E. Serra, A. Borrielli, F. S. Cataliotti, F. Marino, G. A. Prodi, M. Bonaldi, F. Marin, and D. Vitali, *Phys. Rev. A* **89**, 033810 (2014).
- [16] P. Z. G. Fonseca, E.B. Aranas, J. Millen, T.S. Monteiro, P.F. Barker. *arXiv:1511.08482v1 [quant-ph]* (2015).
- [17] Vijay Jain, Jan Gieseler, Clemens Moritz, Christoph Dellago, Romain Quidant, Lukas Novotny, *arXiv:1603.03420*.
- [18] Jamie Vovrosh, Muddassar Rashid, David Hempston, James Bateman, Hendrik Ulbricht, *arXiv:1603.02917*.
- [19] A. Mari and J. Eisert *Phys. Rev. Lett.* **103**, 213603 (2009).
- [20] Daniel Malz, Andreas Nunnenkamp *arXiv:1605.04749* (2016).
- [21] S. Weis, R. Riviere, S. Deleglise, E. Gavartin, O. Arcizet, A. Schliesser, and T. J. Kippenberg, *Science*, **330**, 1520 (2010).
- [22] Zhang-qi Yin, Andrew A. Geraci, and Tongcang Li, *Int. J. Mod. Phys. B* **27**, 1330018 (2013).
- [23] Romero-Isart, O., Juan, M. L., Quidant, R. and Cirac, J. I., *New J. Phys.* **12**, 033015 (2010).
- [24] Chang, D. E. Regal, C. A., Papp, S. B., Wilson, D. J., Ye, J., Painter, O., Kimble, H. J. and Zoller, P., *Proc. Natl Acad. Sci. USA* **107**, 1005 (2010).
- [25] Monteiro, T. S., Millen, J., Pender, G. A. T., Marquardt, F., Chang, D. and Barker, P. F., *New J. Phys.* **15**, 015001 (2013).
- [26] Kiesel, N., Blaser, F., Delić, U., Grass, D., Kaltenbaek, R. and Aspelmeyer, M., *Proc. Natl Acad. Sci. USA* **110**, 14180 (2013).
- [27] Li, T., Kheifets, S. and Raizen, M. G., *Nature Phys.* **7**, 527 (2011).
- [28] Gieseler, J., Deutsch, B., Quidant, R. and Novotny, L., *Phys. Rev. Lett.* **109**, 103603 (2012).
- [29] Millen J, P. Z. G. Fonseca, T. Mavrogordatos, T. S. Monteiro, and P. F. Barker. *Phys. Rev. Lett.* **114**, 123602 (2015)
- [30] See Supplementary Information.